

A min-max optimization algorithm for global active acoustic radiation control

Rong Han ^{*†}, Ming Wu ^{*†}, Kexun Chi ^{*†}, Lan Yin [‡], Hongling Sun ^{*}, Jun Yang ^{*†§}

^{*} Key Laboratory of Noise and Vibration Research, Institute of Acoustics, Chinese Academy of Sciences, China

[†] University of Chinese Academy of Sciences, China

[‡] Institute of Automation, Beijing Information Science and Technology University, China

[§] corresponding author, E-mail: jyang@mail.ioa.ac.cn, Tel: +86-10-82547547

Abstract—Generally, global active noise control is to minimize the sum of the energy of the residual sound field. But on some occasions, we are more concerned that the energy of the residual noise at every direction does not exceed a certain value. In this paper, an algorithm for global active noise control is introduced to achieve a global active acoustic radiation noise control by minimizing the maximum residual sound energy of the far field after active acoustic radiation control. The proposed algorithm adjusts the weights of the secondary sound sources based on the min-max optimization. Simulation results show that the proposed algorithm can reduce the maximum of the far-field residual sound pressure level 2.2 dB more than the maximum of the residual sound pressure level based on the traditional global acoustic radiation control algorithm.

I. INTRODUCTION

Active noise control (ANC) uses loudspeakers to generate sound waves with the same amplitude but opposite phase to the primary noise, thus achieving noise control at certain error points [1], [2]. ANC is divided into local ANC and global ANC [3]. Local ANC reduces the noise at one or several target points, which has lower system complexity. But the space of the noise control is limited [4], [5]. Global ANC controls the noise in a large spatial region. When the primary sound field is complicated such as in highspeed railways and aircrafts, the system with the global ANC is complex and the noise control performance is limited [6], [7]. However, if there is only one primary sound source, global acoustic radiation control can be achieved by placing secondary sound sources of the same magnitude and opposite phase close to the primary sound source to control the radiation noise [3]. Several control strategies are proposed to control the acoustic radiation noise in global spatial region. From 1987 to 1991, Elliott and Nelson studied the noise reduction of a pair of point sources that located in the different positions in the space to study the noise reduction performance of the active acoustic radiation control [8]-[10]. The results show that global acoustic radiation control can only be achieved if the secondary source is placed within half the wavelength of the primary source. Lin discussed the global noise reduction of a piston system mounted on a rigid ball in a free field, and genetic algorithm is performed to choose the position of the secondary sources [11]. Guo studied the control performance of the traditional algorithm for active acoustic radiation control when the error points were at different positions [12]. These methods are to minimize

the sum of the energy of the residual sound field. The total energy of the residual noise field is indeed reduced. However, in some cases, we are concerned that the sound energy at every direction does not exceed a certain value. Gonzalez proposed an adaptive algorithm for minimizing the maximum squared output to achieve noise reductions by restraining the power being supplied to the system [13].

In this paper, to reduce the energy of the residual noise at all points, a min-max optimization is proposed to achieve a global active acoustic radiation control. The remainder of this paper is structured as follows. Chap. 2 derives the traditional algorithm for global active acoustic radiation control. Chap. 3 derives the min-max optimization based on Nelder-Mead algorithm [14] for global active acoustic radiation control. Simulations are conducted in Chap. 4. And Chap.5 concludes this paper.

II. GLOBAL ACOUSTIC RADIATION CONTROL WITH TRADITIONAL ALGORITHM

Global active acoustic radiation control places J secondary sources near the primary source to reduce the energy of the sound in the entire space. An implement of global active acoustic radiation control that four secondary loudspeakers ($J = 4$) are used is shown in Fig. 1. A primary sound source is placed at 5 cm in front of the center of a baffle with 0.6 m long and 3 cm wide, and four secondary sound sources are placed every 10 cm on both sides of the primary sound source. The hard boundary is chosen as the boundary of the baffle.

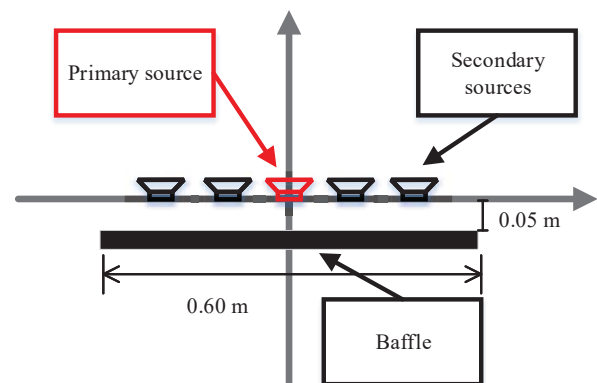


Fig. 1. Implement of the global active acoustic radiation control.

Fig. 2 shows the block diagram of the active acoustic radiation control. x is the reference signal that feeds to the primary source. \mathbf{w} is the weights of the secondary sources. P and S is the primary path from the primary source to the error points, and the secondary paths from the secondary sources to the error points, respectively. Several error microphones are arranged at the error points in the far-field. Suppose the primary noise is periodic noise with 200 Hz. To reduce the noise in the entire spatial, the weights of the secondary sources \mathbf{w} are adjusted. The sum of the energy of the residual sound at the far field $e^2(\theta_i) = \|p(\theta_i) + \mathbf{r}_i^H \mathbf{w}\|_2^2, (i = 1 \sim N)$ is minimized. Therefore, the cost function is written as

$$J_1 = \sum_{i=1}^N E [T_i \cdot e^2(\theta_i)] \quad (1)$$

$$= \sum_{i=1}^N E [T_i \|p(\theta_i) + \mathbf{r}_i^H \mathbf{w}\|_2^2]$$

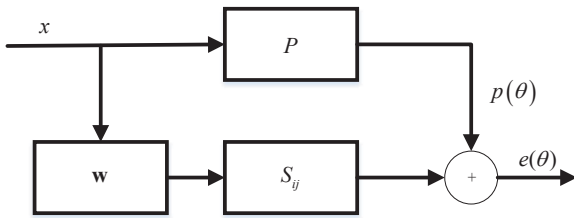


Fig. 2. Block diagram of active acoustic radiation control.

Here, N is the number of the error points. The subscript i denotes the i th position. T_i is the weight of residual noise at the i th error position. $p(\theta_i)$ is the primary noise at the i th error position. θ_i is the the direction of the i th error microphones. The vector of the filtered-x signal $\mathbf{r}_i = [r_{i1}, r_{i2}, r_{i3}, r_{i4}]$ at the i th error position is constructed, where $r_{ij} = x * S_{ij}$ is the filtered-x signal from the j th secondary source to the i th error point, and x is the reference signal. Since the noise to be controlled is periodic, the weights of each secondary sound source $w_j (j = 1 \sim 4)$ are complex values. $\mathbf{w} = [w_1, w_2, w_3, w_4]^T$ is the weight vector of the secondary loudspeakers.

To find the optimal \mathbf{w} which minimizes the cost function J_1 in Eq. (1), calculate its derivative with respect to \mathbf{w} and let the derivative be equal to 0. We expand the cost function J_1 ,

$$J_1 = \sum_{i=1}^N T_i [p^*(\theta_i) p(\theta_i) + \mathbf{w}^H \mathbf{r}_i^* \mathbf{r}_i \mathbf{w} + \mathbf{w}^H \mathbf{r}_i^* p(\theta_i) + p^*(\theta_i) \mathbf{r}_i^H \mathbf{w}] \quad (2)$$

Therefore,

$$\frac{\partial J_1}{\partial \mathbf{w}^*} = \sum_{i=1}^N T_i E (\mathbf{r}_i^* \mathbf{r}_i \mathbf{w} + \mathbf{r}_i^* p(\theta_i)) \quad (3)$$

$$= \sum_{i=1}^N E [\mathbf{R} \mathbf{w} + \mathbf{p}] = 0$$

Here, $\mathbf{R} = \sum_{i=1}^N T_i E [\mathbf{r}_i \mathbf{r}_i^H]$ and $\mathbf{p} = \sum_{i=1}^N T_i E [\mathbf{r}_i^H p(\theta_i)]$. The optimal \mathbf{w}_1 is derived as

$$\mathbf{w}_1 = -\mathbf{R}^{-1} \mathbf{p} \quad (4)$$

In general, $T_i (i = 1, 2, \dots, N)$ are set as 1, i.e. the weights of the components at all error positions are same. If we want to control the noise at one or several certain positions, we can set the T_i that corresponds to these positions to larger values. Thus, the components of cost function at these positions have larger weights.

III. MIN-MAX OPTIMIZATION FOR GLOBAL ACOUSTIC RADIATION CONTROL

The global noise can be controlled by setting all T_i to 1. However, simulations show that the difference between of the maximum and minimum of the residual noise is distinct. We consider that the noise where the residual noise is larger can be reduced much more at the cost of the noise reduction where the residual noise is smaller. On some occasions, we are more concerned that the energy of the residual noise at every direction does not exceed a certain value. It is difficult to adjust T_i by selecting a bigger value at a larger residual sound field and a smaller value at a smaller residual sound field, because there is no effective algorithm to get the optimal values of T_i .

Therefore, we minimize the maximum the energy of the residual sound at the far field after active acoustic radiation control, rather than minimizing the sum of the energy of the residual sound at the far field. Thus, the cost function is written as

$$J_2 = \min \max E [e^2(\theta_i)] \quad (5)$$

$$= \min \|\mathbf{e}_v\|_\infty$$

Here, $\mathbf{e}_v = [E [e^2(\theta_1)], E [e^2(\theta_2)], \dots, E [e^2(\theta_N)]]$. The optimal vector of \mathbf{w}_2 that meets the Eq. (5) is solved. However, this is difficult to find the theoretical optimal solution [15,16]. Therefore, Nelder-Mead algorithm is considered to be used here to find the numerical solution of the Eq. (5) [14,17]. The numerical optimization with Nelder-Mead algorithm is to optimize multiple parameters of real numbers, so a vector \mathbf{z} is constructed as

$$\mathbf{z} = [\text{real}(\mathbf{w}^T), \text{imag}(\mathbf{w}^T)]^T \quad (6)$$

The iterative update of a simplex made of $n + 1$ points are $\mathbf{z}_1, \dots, \mathbf{z}_{n+1}$, and each point is called as a vertice. $\mathbf{z}_2, \dots, \mathbf{z}_{n+1}$ are generated with \mathbf{z}_1 based on the concept of a simplex. Then the optimal \mathbf{z}_{opt} is derived as follows [17]:

Algorithm: Nelder-Mead algorithm

1. Sort the vertices by the values of the cost function. Suppose $J_2(\mathbf{z}_1) \leq J_2(\mathbf{z}_2) \leq \dots \leq J_2(\mathbf{z}_{n+1})$.
2. Calculate \mathbf{z}_0 , the centroid of the vertices except \mathbf{z}_{n+1} .
3. Calculate the reflected vertex $\mathbf{z}_r = \mathbf{z}_0 + \alpha(\mathbf{z}_0 - \mathbf{z}_n)$. If $J_2(\mathbf{z}_1) \leq J_2(\mathbf{z}_r) \leq J_2(\mathbf{z}_{n+1})$, $\mathbf{z}_{n+1} = \mathbf{z}_r$ and go to step 1. If $J_2(\mathbf{z}_r) \leq J_2(\mathbf{z}_1)$, $\mathbf{z}_e = \mathbf{z}_0 + \gamma(\mathbf{z}_r - \mathbf{z}_0)$. Then if $J_2(\mathbf{z}_e) \leq J_2(\mathbf{z}_r)$, $\mathbf{z}_{n+1} = \mathbf{z}_e$, else $\mathbf{z}_{n+1} = \mathbf{z}_r$, and go to step 1.
4. Calculate $\mathbf{z}_c = \mathbf{z}_0 + \rho(\mathbf{z}_{n+1} - \mathbf{z}_0)$, if $J_2(\mathbf{z}_c) \leq J_2(\mathbf{z}_{n+1})$, $\mathbf{z}_{n+1} = \mathbf{z}_c$, and go to step 1.
5. Replace all vertices except \mathbf{z}_1 , and go to step 1.
6. Stop when the standard deviation of the values of the cost function is below some tolerance.

Here, α, γ, ρ and σ are the reflection, expansion, contraction and shrink coefficients, respectively [17]. Since the local optimum values of the optimization problem near the initial value is searched, given different initial values will result in different optimal values of \mathbf{w}_2 . To control the radiation noise in the entire spatial, the initial value is set as the optimal values of \mathbf{w}_1 derived as Eq. (4).

IV. SIMULATIONS AND RESULTS

Simulations are conducted in the 2-D sound field to show the noise control performance with the two algorithms derived in Chap. 2 and Chap. 3. One primary sound resource and four secondary sound resources placed before a baffle which is shown in Fig. 1 are implemented at the center of the space. There is no reflection in the surrounding space. 36 error points are equally spaced at $R = 10$ m as shown in Fig. 3. The 180 transfer functions from the primary and secondary loudspeakers to the error points (5 sound sources to 36 error points) are obtained with the multiphysics simulation software, Comsol.

The primary sound resource generates periodic noise with 200 Hz. When the optimal weight of \mathbf{w} is obtained with Eq. (4), the primary noise in the space and the 36 error points are shown in Fig. 4. The noise radiated by the primary sound resource can be effectively controlled by active acoustic radiation control. The noise deduction is 40~70 dB at these 36 error positions.

However, it is also found that the sound pressure level at the 20° in the residual sound field is 25 dB more than that at the 40° with the traditional algorithm. Difference between the maximum and minimum of the sound pressure level of the residual noise with the traditional algorithm is 27 dB. The optimal weight based on the min-max optimization is calculated with the initial value that obtained with Eq. (4). The residual sound field with the traditional algorithm and min-max optimization is shown in Fig. 5 and Fig. 6. The maximum sound pressure level of the residual noise at 20° is 2.2 dB less than that with the traditional algorithm. Difference between the maximum and minimum of the sound pressure level of the residual noise with the min-max optimization is 9 dB, which is 18 dB less than with the traditional algorithm.

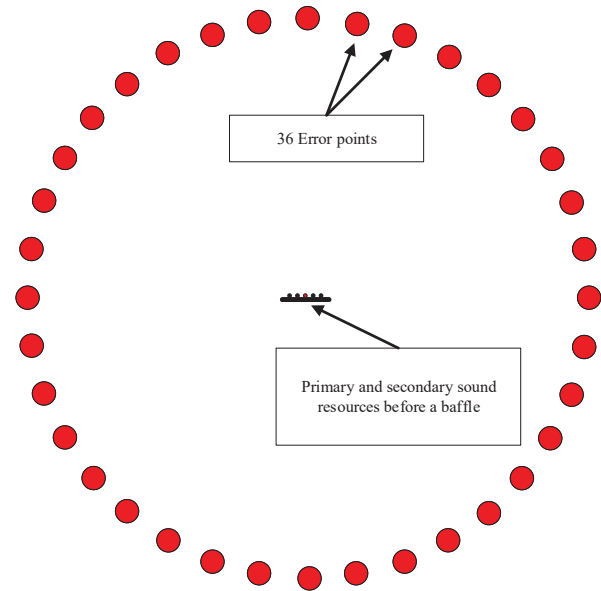


Fig. 3. Implement of the global active acoustic radiation control.

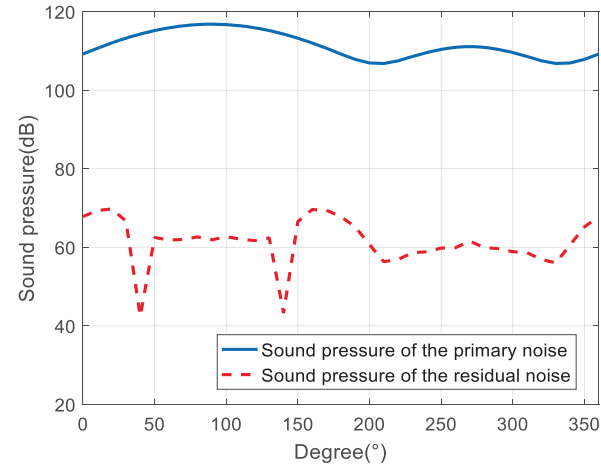


Fig. 4. Sound pressure level before and after the active acoustic radiation control.

TABLE I
VALUES OF COST FUNCTION WITH THE TRADITIONAL ALGORITHM AND MIN-MAX OPTIMIZATION.

| values of cost function | J_1 | J_2 |
|-------------------------|----------------------|----------------------|
| traditional algorithm | 9.1396×10^7 | 9.4664×10^6 |
| min-max optimization | 1.1374×10^8 | 5.7022×10^6 |

The values of cost function when the weight of the secondary sources, \mathbf{w} , are calculated with the traditional algorithm and min-max optimization, respectively, are listed in Table. 1. Although the values of J_1 is increased with the min-max optimization, the values of J_2 is decreased.

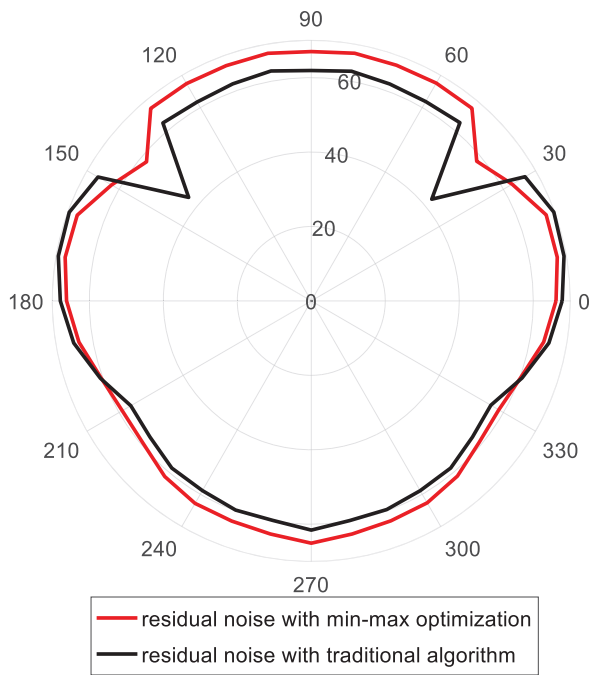


Fig. 5. Polar map of the sound pressure level of the residual noise at $R = 10$ m with traditional algorithm and min-max optimization. (Unit: dB)

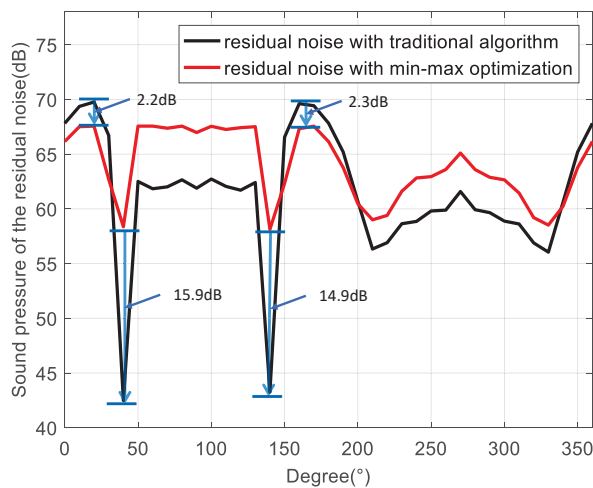


Fig. 6. The sound pressure level of the residual noise at $R = 10$ m with traditional algorithm and min-max optimization

V. CONCLUSIONS

In order to control the global acoustic radiation noise, an algorithm for global acoustic radiation control is introduced by minimizing the maximum residual sound energy of the far field after active acoustic radiation control. The proposed algorithm adjusts the weights of the secondary sound sources based on the min-max optimization. The optimal weight derived as the traditional algorithm is set as the initial value in the proposed algorithm. Simulation results show that the difference between the maximum and minimum of the sound pressure level of the residual noise with the min-max optimization is 18 dB

less than with the traditional algorithm. The maximum of the residual noise with traditional algorithm is 2.2 dB less than that with the min-max optimization.

ACKNOWLEDGMENT

This work is supported by the National Key Research and Development Program of China (Grant No. 2016YFB1200503) and the National Natural Science Foundation of China (Grant No. 11474306, No. 11404367, and No. 11474307).

REFERENCES

- [1] S. M. Kuo and D. R. Morgan, "Active noise control: A tutorial review," *Proceedings of the IEEE*, vol. 87, pp. 943–973, 1999.
- [2] Y. Kajikawa, W.-S. Gan, and S. M. Kuo, "Recent advances on active noise control: Open issues and innovative applications," *APSIPA Transactions on Signal and Information Processing*, vol. 1, p. e3, 2012.
- [3] C. Hansen, S. Snyder, X. Qiu, L. Brooks, and D. Moreau, *Active Control of Noise and Vibration*, 2nd ed. CRC Press, 2012.
- [4] C. Lei, J. Xu, J. Wang, C. Zheng, and X. Li, "Active Headrest with Robust Performance Against Head Movement," *Low Frequency Noise, Vibration and Active Control*, vol. 34, pp. 233–250, 2015.
- [5] S. J. Elliott, W. Jung, and J. Cheer, "Head Tracking Extends Local Active Control of Broadband Sound to Higher Frequencies," *Scientific Reports*, vol. 8, no. 1, p. 5403, 2018.
- [6] R. Han, M. Wu, C. Gong, S. Jia, T. Han, H. Sun, and J. Yang, "Combination of Robust Algorithm and Head-Tracking for a Feedforward Active Headrest," *Applied Sciences*, vol. 9, no. 9, p. 1760, 2019.
- [7] T. Haase, O. Unruh, S. Algermissen, and M. Pohl, "Active control of counter-rotating open rotor interior noise in a Dornier 728 experimental aircraft," *Journal of Sound and Vibration*, vol. 376, pp. 18–32, 2016.
- [8] S. J. Elliott, P. Joseph, P. A. Nelson, and M. E. Johnson, "Power output minimization and power absorption in the active control of sound," *The Journal of the Acoustical Society of America*, vol. 90, no. 5, pp. 2501–2512, 1991.
- [9] P. Nelson, A. Curtis, S. Elliott, and A. Bullmore, "The minimum power output of free field point sources and the active control of sound," *Journal of Sound and Vibration*, vol. 116, no. 3, pp. 397–414, 1987.
- [10] P. A. Nelson and S. J. Elliott, *Active Control of Sound*. Academic Press, 1991.
- [11] Z. Lin, J. Lu, C. Shen, X. Qiu, and B. Xu, "Active control of radiation from a piston set in a rigid sphere," *The Journal of the Acoustical Society of America*, vol. 115, no. 6, pp. 2954–2963, 2004.
- [12] G. Qin, "A study on error microphone location for active sound radiation control," Ph.D. dissertation, Nanjing University, Nanjing, 2018.
- [13] A. Gonzalez, A. Albiol, and S. J. Elliott, "Minimization of the maximum error signal in active control," *IEEE Transactions on Speech and Audio Processing*, vol. 6, no. 3, pp. 268–281, 1998.
- [14] J. A. Nelder and R. Mead, "A Simplex Method for Function Minimization," *The Computer Journal*, vol. 7, no. 4, pp. 308–313, 1965.
- [15] S. Boyd and L. Vandenberghe, *Convex Optimization*. New York, NY, USA: Cambridge University Press, 2004.
- [16] H. Rafique, M. Liu, Q. Lin, and T. Yang, "Non-Convex Min-Max Optimization: Provable Algorithms and Applications in Machine Learning," *arXiv:1810.02060 [cs, math]*, 2018.
- [17] R. M. Lewis, A. Shepherd, and V. Torczon, "Implementing Generating Set Search Methods for Linearly Constrained Minimization," *SIAM Journal on Scientific Computing*, vol. 29, no. 6, pp. 2507–2530, 2007.